Polymer Chemistry

Photo-curing of 4-arm coumarin-functionalised monomers to form highly photoreversible crosslinked epoxy coatings

Journal:	*Polymer Chemistry*
Manuscript ID	PY-ART-12-2018-001767.R1
Article Type:	Paper
Date Submitted by the Author:	17-Mar-2019
Complete List of Authors:	Hughes, Timothy; Monash University, School of Chemistry Simon, George; Monash University, Materials Science and Engineering Saito, Kei; Monash University, Centre for Green Chemistry, School of Chemistry

Journal Name

ARTICLE

Photocuring of 4-arm coumarin-functionalised monomers to form highly photoreversible crosslinked epoxy coatings

T. Hughes,[a] G. P. Simon[b*] and K. Saito[a*]

Received 00th January 20xx,
Accepted 00th January 20xx

DOI: 10.1039/x0xx00000x

www.rsc.org/

Highly photoreversible and photo-curable epoxy-based network polymers suitable for coating applications were produced by the synthesis of two coumarin-functionalised monomers. Three polymers were formed from the synthesised monomers: two of which are the monomers polymerised separately, with the third being a polymerised mixture of a 50 mol% blend of the two monomers. Through the irradiation with 365 nm UV light, high strength crosslinked networks were formed that exhibited thermal and mechanical properties similar to common commercial coating materials. These photopolymers were also tested for their photoreversible nature in response to different wavelengths of UV light using several analytical techniques as well as characterising them by studying their photoinduced solubility and examining their self-healing performance. These results demonstrated the ability to tune the polymers properties, such as self-healing ability, by the monomer content as the mixed polymer exhibited exceptional healing performance and mechanical properties.

Introduction

Photopolymerisation is not a new concept, having been investigated for over 150 years and has been viewed as a green alternative to thermal processes due to the ability to form polymers at room temperature utilising light irradiation to not only reduce the energy cost of polymerisation but allow for the use of more robust polymers as coatings on sensitive substrates[1-3]. Photoreversible polymers have emerged as a more beneficial approach as they not only do not require the use of photoinitiators for polymerisation but also possess the ability to revert to small oligomers and in some cases the original polymer building blocks to allow for many interesting capabilities such as precise reaction control, recyclability, self-healing, reworkability and property tuning.[4-16]

Photoreversible polymers are commonly created by the addition of reversible units into a polymer structure either in the monomer that is polymerised by another means or as the polymerisation mechanism itself, this allows the polymer structure to be reversibly cleaved to form smaller units capable of flowing that give rise to the many properties mentioned above.[17-20] Common photoreversible mechanisms are based on dynamic covalent chemistry and tend to yield hard, mechanically robust polymers ideal for structural or coating applications.[21-23] Some of the most common photodynamic covalent chemistries are the photocycloaddition of anthracene, coumarin, cinnamic acid and thymine or the reversible photo-cleavage of disulfides, allyl sulphide and trithiocarbonates.[24-27]

Using this principle, small photo-curable monomers were synthesised to allow the utilising coumarin photocycloaddition for the reversible photopolymerisation. Coumarin was chosen for the high efficiency of the reversible mechanism as well as for being readily-available in many functionalised forms.[28-30] It is also advantageous because of its proven capability for the use of sunlight as the stimulus for the photocycloaddition.[31-34] The monomer structure synthesised was a 4-armed 'cross-like' structure with the coumarin moieties positioned at the end of each arm as this would allow a high degree of crosslinking by irradiation with 365 nm UV light ensuring a hard, rigid material would result. This 4-armed structure has been previously implemented successfully to form crosslinked polymers for use as hydrogels by Truong *et al.*[35, 36] however we form smaller epoxy-based monomers to allow a much greater crosslink density to give the rigid coating material. As the coumarin dimerisation is photoreversible, the polymerisation can be reversed with 254 nm UV light to return the material to a near monomeric state yielding a decrosslinked material which can be reworked with heating or recycled by dissolution, redeposition and recrosslinking by the initial 365 nm UV light treatment.[37-39]

These 4-arm coumarin monomers (4ACM) were synthesised by the epoxylation of coumarin and the subsequent reaction with diamine chains of varying, but relatively short, chain lengths to ensure a high strength polymer. Through the photocuring of these monomers both individually and in a 50 mol% mixture, three polymers were created. The photopolymers all exhibited a high degree of photoreversibility and an interesting range of thermal and mechanical properties.

As the synthesis of these monomers is simple and the polymers produced were found to be ideal for use as coatings, there is great potential for creation of a larger suite of similarly structured monomers and polymers suitable for different commercial applications.

[a] School of Chemistry, Monash University, Clayton, VIC 3800, Australia, e-mail: kei.saito@monash.edu; Fax: +6139905851; Tel: +61399054600.
[b] Department of Materials Science & Engineering, Monash University, Clayton, VIC 3800, Australia. E-mail: george.simon@monash.edu; Fax: +61 399054934; Tel: +61 399054936.

Experimental

Materials

7-hydroxycoumarin (Sigma-Aldrich), epichlorohydrin (Sigma-Aldrich), 1,6-diaminohexane (Sigma-Aldrich) and 1,10-diaminodecane (Fluka) were used as supplied by their respective suppliers.

Equipment/Characterisation

Photoreactions were conducted in a UVP UV crosslinker (CL-1000L 365 nm and CL-1000 254 nm). ^{1}H NMR and ^{13}C NMR were measured on Bruker DRX 400 spectrometer. Mass and IR spectra were recorded on Agilent 6120 Quadrupole LC/MS and Agilent Cary 630 FTIR spectrometers, respectively. Differential scanning calorimetry (DSC) analysis and thermogravimetric analysis (TGA) were performed using a PerkinElmer DSC8000 and Mettler TGA/DSC1 STAR system respectively. Photo-DSC analysis was collected on the NETZSCH Photo-DSC 204 F1 Phoenix®. UV-vis spectra were collected using a Shimadzu UV-1800 spectrometer. Molecular weight determinations were made using of a Tosoh High Performance EcoSEC HLC-8320 GPC System calibrated with a polystyrene standard and equipped with a TSKgel Alpha guard column and two analysis columns in series: TSKgel Alpha-4000 (400 Å pore size) and TSKgel Alpha-2500 (125 Å pore size). Hardness measurements were collected on a Struers Duramin A300 durometer. Optical microscope images were taken with an Olympus GX51.

Synthesis of 4ACM-6 and 4ACM-10 photo-curable monomers

Synthesis of 7-(oxiran-2-ylmethoxy)-2H-chromen-2-one (EMC) [40, 41]

7-hydroxycoumarin (3.27 g, 20.2 mmol) was suspended in ethanol (100 mL) to which was added 4.5 M KOH (5 mL, 22.5 mmol) and the mixture stirred at room temperature for 35 minutes to form a bright orange solution. Epichlorohydrin (20 mL, 183 mmol) was added and the solution stirred under heavy reflux at 95 °C for 2.5 hours. The reaction mixture was allowed to cool to room temperature and the resultant mixture filtered. The filtrate was evaporated to dryness and the residue dissolved in ethyl acetate (100 mL), washed with water (3x40 mL), dried over $MgSO_4$, filtered and the filtrate evaporated to dryness. The resultant solids were then recrystallised from ethanol (8 mL) to afford the desired EMC in high purity (2.31 g, 10.6 mmol, 53%); ^{1}H NMR (400 MHz, $CDCl_3$) δ 2.78 (m, 1H), 2.94 (t, 1H), 3.38 (m, 1H), 3.96 (dd, 1H), 4.33 (dd, 1H), 6.25 (d, 1H), 6.82 (d, 1H), 6.87 (dd, 1H), 7.37 (d, 1H), 7.63 (d, 1H) ppm; ^{13}C NMR (100 MHz, $CDCl_3$) δ 44.7, 49.9, 69.4, 101.8, 113.1, 113.2, 113.6, 129.1, 143.5, 155.9, 161.2, 161.7 ppm; IR (ATR) 3089, 2930, 1707, 1610, 1506, 1119, 1021, 907, 827 cm^{-1}; MS (ESI) m/z (%) 217.05 ([M-H]$^-$, 100); m.p. = 120.2 °C.

Synthesis of 7,7',7'',7'''-(((hexane-1,6-diylbis(azanetriyl))tetrakis(2-hydroxypropane-3,1-diyl))tetrakis(oxy))tetrakis(2H-chromen-2-one) (4ACM-6)

EMC (0.406 g, 1.86 mmol) and 1,6-diaminohexane (52.6 mg, 0.45 mmol) were melted together at 130 °C, stirred for 48 hours and the resultant viscous liquid cooled to room temperature. The residue was stirred in chloroform, filtered under vacuum and evaporated to afford pure 4ACM-6 as a bright yellow powder (0.42 g, 0.43 mmol, 92%); ^{1}H NMR (400 MHz, d^6-DMSO) δ 1.33 (s br, 3H), 1.53 (s br, 3H), 2.73 (m br, 8H), 4.05 (m, 16H), 6.24 (d, 4H), 6.80 (m, 8H), 7.35 (d, 4H), 7.61 (d, 4H) ppm; ^{13}C NMR (100 MHz, $CDCl_3$) δ 27.0, 57.6, 58.3, 63.4, 68.3, 69.1, 70.1, 70.7, 86.2, 101.5, 113.2, 129.0 143.4, 155.7, 161.4 ppm; IR (ATR) 3406, 3084, 3012, 2930, 2859, 1704, 1607, 1556, 1506, 1279, 1229, 1118, 1025, 830 cm^{-1}; MS (ESI) m/z (%) 989.37 (M^+, 100).

Synthesis of 7,7',7'',7'''-(((decane-1,10-diylbis(azanetriyl))tetrakis(2-hydroxypropane-3,1-diyl))tetrakis(oxy))tetrakis(2H-chromen-2-one) (4ACM-10)

EMC (0.30 g, 1.38 mmol) and 1,10-diaminodecane (59.4 mg, 0.35 mmol) were melted together at 130 °C and the melt stirred for 48 hours to produce a viscous liquid which was cooled to room temperature. The resultant residue was dissolved in chloroform, filtered under vacuum and evaporated to afford pure 4ACM-10 as a bright yellow powder (0.34 g, 0.32 mmol, 94%); ^{1}H NMR (400 MHz, $CDCl_3$) δ 1.24 (d br, 12H), 1.53 (d br, 4H), 2.70 (d br, 4H), 2.89 (m, 8H), 4.05 (s, 8H), 4.20 (d, 4H), 6.23 (d, 4H), 6.83 (m, 8H) ppm, 7.34 (m, 4H), 7.36 (d, 4H); ^{13}C NMR (100 MHz, $CDCl_3$) δ 27.2, 29.3, 56.1, 57.6, 58.3, 67.3, 67.9, 70.7, 101.6, 113.0, 128.9, 143.4, 155.7, 161.2, 161.8 ppm; IR (ATR) 3406, 3084, 2924, 2851, 1703, 1607, 1556, 1507, 1279, 1228, 1119, 1023, 830 cm^{-1}; MS (ESI) m/z (%) 1043.42 ([M-H]$^-$, 100).

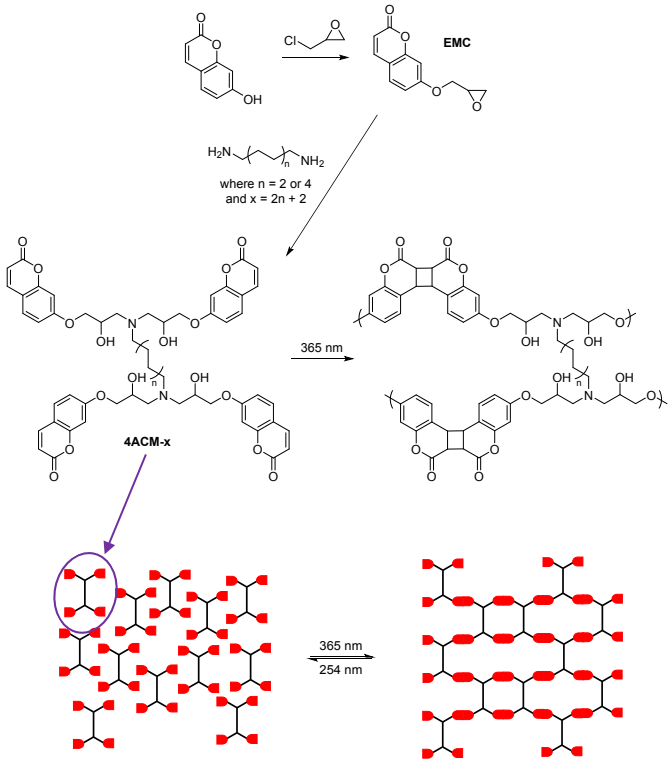

Figure 1: Synthesis scheme of the two 4-armed photo-curable coumarin monomers (4ACM-6 and 4ACM-10) and subsequent polymerisation by 365 nm UV light irradiation as well as an illustration of the photoreversible polymerisation.

Preparation of photopolymers

Using the synthesised monomers, three polymers were produced: two of which were each monomer polymerised separately (4ACM-6 and 4ACM-10 polymers) and the third was the two monomers polymerised together in a 50:50 mole mixture (4ACM-m polymer).

The monomer solutions in chloroform (ca. 0.05 M) were cast on glass slides and dried at 40 °C for upwards of 3 hours to form thin films. These films were irradiated with 365 nm UV light under air at room temperature, unless otherwise stated, for up to 8 hours to induce the coumarin photoreaction, and produce the desired crosslinked polymers films.

4ACM-6: IR (ATR) 2933, 2875, 1737, 1610, 1584, 1506, 1232, 1157, 1103, 1023, 833, 747 cm^{-1}.

4ACM-10: IR (ATR) 2922, 2859, 1735, 1615, 1587, 1506, 1232, 1157, 1105, 1023, 833, 747 cm^{-1}.

4ACM-m: IR (ATR) 2929, 2855, 1737, 1614, 1586, 1506, 1232, 1157, 1105, 1025, 833, 743 cm^{-1}.

For different analyses, different samples were required. For the UV-vis spectroscopy sample the monomers were spin-coated on small quartz squares from the chloroform solutions to form very thin films. Thicker samples were needed for the IR spectroscopy and hardness analysis to ensure no influence by the substrate, these were formed by depositing the monomer solutions on a glass slide with a pipette, allowing some time for the monomer to dry and then deposition of more solution which was repeated until a sufficient sample thickness was reached. For these thicker samples the 365 nm irradiation time was increased to around 16 hours to ensure adequate crosslinking of the polymer throughout the depth of the sample.

Results and Discussion

Several analytical techniques were used to monitor the occurrence of the desired reversible photoreaction, investigate thermal behaviour and evaluate the performance and potential for application of the resultant photopolymers.

Photocuring of the synthesised monomers

A sample of each photopolymer was formed by dissolving the monomers in chloroform, depositing the solution on a glass slide and drying the samples in a vacuum oven at 40 °C. The samples were then irradiated with 365 nm UV light to cause polymerisation, forming a crosslinked polymer network. This process was monitored by IR and UV-vis spectroscopy to determine the time required for polymerisation to cease and to confirm the polymerisation mechanism by observation of the signals for key functional groups.

As can be seen from the IR spectra in Figure 2, S2 and S3, the carbonyl signal of the coumarin moieties inside the monomers shifts significantly from ca. 1705 cm^{-1} to ca. 1735 cm^{-1} which is commonly observed when coumarin is dimerised. The carbon-carbon double bond of the coumarin visible at ca. 1558 cm^{-1} is also seen to decrease significantly after irradiation. This confirmed that the coumarin double bonds of the monomers were reacting due to the 365 nm irradiation.[30]

UV-vis spectroscopy was used to determine the extent to which the polymerisation occurred to ensure a crosslinked network was being formed. Quantification of the polymerisation reaction was achieved through monitoring and comparison of the coumarin double bond absorbance signal at 321 nm.[30] Figure 2a, S2a and S3a show the spectra of all three monomer systems when subjected to 365 nm irradiation, the coumarin double bond signal at 321 nm is seen to decrease significantly for each, and stops decreasing after 2.06, 3.43 and 2.06 J/cm^2 of irradiation respectively, indicating the reaction of the coumarin double bond. There is, however, some absorbance still present at 321 nm which indicate the unreacted

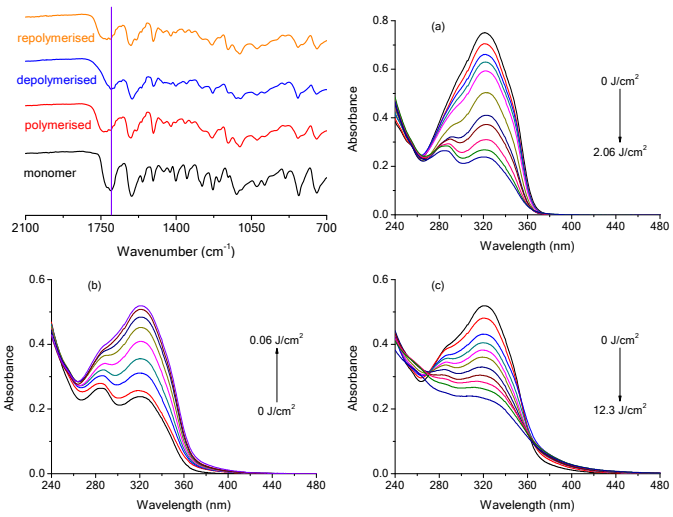

Figure 2: Monitoring of the photoreversibility of the crosslinked polymer 4ACM-6 by IR spectrometry (top left) and by UV-vis spectroscopy through the two stages: (a) polymerisation, (b) depolymerisation and (c) repolymerisation.

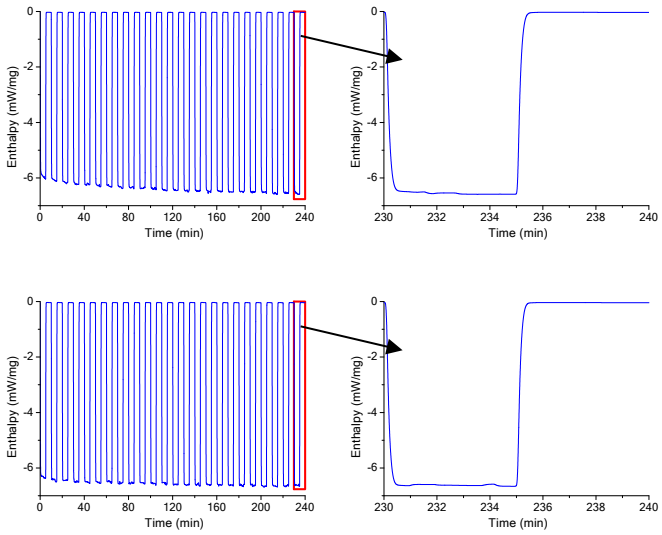

Figure 3: Photo-DSC analysis of the photocuring of the two monomers 4ACM-6 (top) and 4ACM-10 (bottom) for all 24 runs (left) and a magnified view of only the final run (right). Each run consisted of 5 minutes of 365 nm UV light irradiation followed by 5 minutes of no irradiation. The irradiation was provided by a mercury UV lamp of 4 W/cm^2 intensity with a spectral range of 320 – 500 nm.

coumarin double bonds. The percentage of coumarin units reacted were calculated to be 67%, 66% and 73% for 4ACM-6, 4ACM-10 and 4ACM-m, respectively, resulting in crosslinked density of 2.7, 2.5 and 2.9 mmol of crosslinks per gram of polymer. These values were calculated under the assumption that a 100% reaction of the coumarins would result in a zero absorbance at 321 nm. It is important to note that due to steric hindrance, the decreasing mobility of the chains as the crosslinked network forms, and the need for strict alignment of the coumarin double bonds for reaction to occur, it is unlikely that all the coumarin sites will react, however a high degree of crosslinking was still obtained.

Samples of 4ACM-6 and 4ACM-10 were analysed by Photo-DSC wherein the monomer samples were irradiate with light from 320 – 500 nm and the heat of reaction measured. The samples were irradiated with 4 W/cm^2 for 5 minutes periods whilst under a nitrogen atmosphere at 30 °C, the DSC curves for this analysis can be seen in Figure 3. For both the monomers a strong exothermic change in enthalpy to the irradiation can be seen confirming the reaction upon irradiation with >320 nm UV light. As the coumarin double bonds are known to be active >320 nm this enthalpy response can be attributed to the polymerisation of the monomers via coumarin dimerisation. The enthalpy of the reaction of both monomers increases slightly over time, both plateauing at around 1.95 J/mg which is expected as they both contain four reactive sites per monomer and with the molecular weight being no more than 6% different, the reactive sites per unit mass will also be of similar value and thus similar reaction enthalpies should be observed. The reaction was seen to cease immediately after the irradiation is stopped, demonstrating the precise reaction control of this type of photopolymerisation. For a photoinitiator polymerisation system, tailing would occur indicating the continued radical polymerisation after irradiation was ceased.

Thermal property analysis of photopolymers

After the polymerisation process was confirmed, thermal properties of the polymers could be evaluated. The decomposition temperature was determined for each polymer with TGA, with the degradation curves displayed in Figure S1. All three polymers displayed similar decomposition temperatures, as expected due to the structural similarity, with each commencing at ca. 250 °C, which is far in excess of the common upper limit service temperature of epoxy systems of 150 °C.[42]

To determine whether the materials were suitable for the proposed coating applications, the glass transition temperature (T_g) of the three systems was measured using DSC and the results shown in Table 1 & Figure S4. As expected, the T_g of the more flexible 4ACM-10 polymer is the lowest of the three and the T_g of 4ACM-m falls almost exactly in-between, as it is a 50 mol% mixture of the two monomers. All three polymers possess T_g values suitable for differing coating applications, with the T_g values of the 4ACM-10 and 4ACM-6 polymers being almost identical to that of the flexible coating material PET at 65 °C and the more rigid PMMA at 105 °C, respectively.[43, 44]

Depolymerisation and repolymerisation of photopolymers

To ensure the polymers exhibited the desired photoreversible character, a photoreversibility study was conducted on all the synthesised polymers utilising IR and UV-vis spectroscopy (Figure 2, S2 and S3) during the depolymerisation with 254 nm and repolymerisation with 365 nm.

As seen above, the dimerisation of the coumarin sites during polymerisation was followed using FTIR by the blueshift of the carbonyl signal at 1705 cm^{-1} and the disappearance of the double bond signal at 1558 cm^{-1} and thus these signals can again be monitored to follow the depolymerisation and subsequent repolymerisation. For all three systems exposed to 254 nm irradiation, the carbonyl signal shifts back to the original position of 1705 cm^{-1} and is accompanied by a re-emergence of the signal at 1558 cm^{-1} indicating that depolymerisation is occurring. Under 365 nm irradiation all three systems behave similarly, with the carbonyl shifting to the original position and the double bond signal decreasing significantly. It was found that the effect on the 4ACM-6 system was most pronounced, as the spectra of the original polymer and the repolymerised polymer are almost identical, whereas the other two systems show noticeable variations; this suggests a greater relative extent of repolymerisation in the 4ACM-6 system.

The UV-vis spectra show that all the polymers follow the expected trend for the two processes; the coumarin double bond signal at 321 nm increases during depolymerisation and decreases again during repolymerisation.[30] By comparison of the absorbance values of this signal the percentage of coumarin sites reacted can be determined. During depolymerisation it can be seen that a significant portion of coumarin dimers are cleaved, 58% of the dimers are cleaved for 4ACM-6, 61% for 4ACM-10 and 81% for 4ACM-m. Also of note, the decrosslinking requires much less irradiation as 254 nm is a higher energy wavelength than 365 nm, thus less irradiation is required to induce the same energy change in the system. There is also less 'wasted' energy as with the polymerisation, light that strikes coumarins that are not in the correct alignment will not illicit a dimer, hence that light is 'wasted'. The higher depolymerisation exhibited by the 4ACM-m polymer could be attributed to the disordered structure, that results from mixing of the two monomers that have different structures. This could introduce strain that is not present in the single monomer polymers, leading to more favourable cleavage of the coumarin dimers. For the repolymerisation stage there was a 96%, 90% and 88%, respective decrease in the absorbance of the signal, indicating the re-dimerisation of almost all the cleaved coumarin dimers.

The depolymerisation of the polymers was further investigated with a solubility study which involved submerging of samples of the polymers in chloroform whilst irradiating with

Table 1: Glass transition temperatures (T_g) of the three polymers in the virgin polymer state and after depolymerisation, as measured by DSC using a 10 °C/min heating rate.

	4ACM-6	4ACM-10	4ACM-m
Polymerised	104 °C	64 °C	87 °C
Depolymerised	22 °C	13 °C	-5 °C

254 nm UV light (Figure 4). During depolymerisation, the crosslinked polymer becomes oligomeric with some monomers which, as they are no longer crosslinked, are soluble and hence will dissolve in a solvent. The mass of the samples were monitored as a function of irradiation time and all polymers were found to completely dissolve with similar irradiation doses. This test successfully demonstrates the decrosslinking of the polymer, as well as indicates an initial high degree of crosslinking for all three polymers as before the 254 nm irradiation the soluble fraction of the polymer was very small. This initial soluble portion can be attributed to unreacted monomers and oligomers that were not incorporated into the crosslinked structure. After the samples were completely solubilised by irradiation with 254 nm UV light, the solutions were dried and analysed by GPC. The spectra all show a broad peak, indicating a wide range of molecular weights of the liberated soluble polymers were obtained from the decrosslinking. This was as expected since the polymer will randomly cleave and with incomplete depolymerisation leads to the wide range of molecular weight of the liberated material. The GPC trace of the depolymerised 4ACM-m shows a lower average molecular weight than the other systems. This agrees strongly with the UV-vis study earlier, which indicates that more coumarin dimers are cleaved during depolymerisation for the 4ACM-m polymer than in the other two systems. As more coumarin dimers are broken, fragments of lower molecular weight are obtained.

To further characterise the depolymerisation, the polymer solutions were evaporated to remove all solvent and analysed by DSC to give a depolymerised T_g, the values from the DSC curves are displayed in Table 1 & Figure S4. As expected, the T_g values are much lower than for crosslinked samples, with the depolymerisation process leading to small polymeric and oligomeric fragments. The glass transition temperatures value for the more flexible 4ACM-10 polymer were lower than that of 4ACM-6, however unexpectedly the value for the 4ACM-m polymer is lower than both the single monomer polymers. The low depolymerised T_g of 4ACM-m compared to the other two systems again agrees strongly with the previous analysis. The GPC of the depolymerised 4ACM-m material was of lower molecular weight than the others which, given the similarity in structure of the polymers, results in a lower depolymerised T_g. However as this value is much lower than expected further factors must be having an effect. One factor is possibly due to the disordered structure, that was discussed above in relation to the higher depolymerisation, resulting in less interactions, specifically π-π interactions of the coumarin moieties, between the depolymerised chains leading to an increase in free volume and thus lowering of the depolymerised T_g.

Mechanical property analysis

The key mechanical property of interest for a coating material is hardness as this is related to a coatings scratch resistance with a higher value indicating a better protection of the underlying substrate. As these polymers are reversible, hardness testing can also allow further investigation of the reversibility mechanism, as the polymers will likely soften when they are depolymerised with 254 nm UV light and subsequently harden when repolymerised with 365 nm UV light. To measure this, samples of each polymer were coated on glass slides and the hardness measured with a durometer at three different stages; after polymerisation, after depolymerisation and after repolymerisation.

As can be seen in Table 2, all three polymers exhibit hardness suitable for use as a coating material, as the values were comparable or above the 20 HV of the common automotive coating material PMMA.[45, 46] As expected upon depolymerisation, there was a significant softening of the polymers and with the repolymerisation stage the polymers were seen to almost completely return to their original hardness. The percentage of hardness regained for 4ACM-6, 4ACM-10 and 4ACM-m were 85%, 78% and 85% respectively, which agree strongly with the photoreversibility study which for polymers suggested around 90% reformation of the broken coumarin dimers during repolymerisation. With the high degree of recovery of the hardness upon repolymerisation the polymers are still suitable for use as a coating, indicating the photoreversible mechanism would not diminish the polymers capabilities. This result suggests that any processing defects in the polymers could be healed by this mechanism, with little compromise in polymer performance.

Self-healing of crosslinked photopolymers

One beneficial characteristic of photoreversible polymers is the potential for self-healing by the transition from a rigid crosslinked structure to small oligomeric or monomeric material that can flow and heal imposed damage. This property would be ideal for a coating material, as imposed scratches or cracks could be healed without replacement of the coating, extending the lifetime of the coating and reducing the environmental impact of the material by reduction of waste arising from the common coating repair methods of buffing or recoating.[47-51]

Our group has previously synthesised self-healing polymers

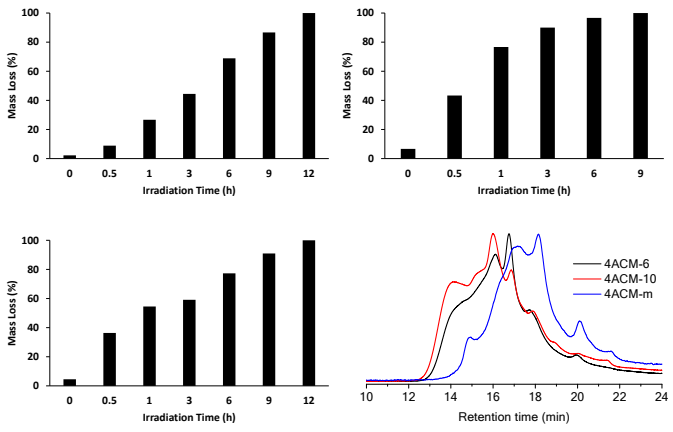

Figure 4: Mass loss from the crosslinked polymers during irradiation with 254 nm UV light for 4ACM-6 (top left), 4ACM-10 (top right) and 4ACM-m (bottom left) and the GPC chromatograms of the soluble portion of the polymers after irradiation (bottom right). UV light doses of 8.2 J/cm^2, 6.17 J/cm^2 and 8.2 J/cm^2 respectively.

created through various approaches.[10-12,52] In our previous designs thermally-cured polymers were healed with heat or light by the cleavage of a reversible unit within a functionalised crosslinker. This design was unique at the time and led to a large suite of healable polymers. However in this 4-arm design the polymer is able to cleave to much smaller fragments by 254 nm UV light irradiation, as the previous designs gave the transition from thermoset to thermoplastic whereas this current design can transition from thermoset to monomeric or oligomeric scale materials. From our experience this should result in greater self-healing performance as the fragments can flow and fill the damaged site with greater ease. Considering the analysis performed on the 4ACM polymers above, the potential for self-healing is great due to the low T_g values observed for the depolymerised structures, which suggests it should be able to flow at room temperature, and thus may outperform the previous design in healing capability.[12,52] With the relatively small monomer compared to other previously reported photopolymerisable self-healing polymers,[53] the resultant polymers exhibit higher crosslink densities and great mechanical properties, such as hardness and rigidity, which allows them to function as photopolymerisable coatings as well as have the potential for self-healing. With all these benefits taken into account, the 4ACM polymers represent a significant advantage over previous photo-healable polymer designs due to their superior mechanical properties and high photoreversibility.

The produced photopolymers were tested for their self-healing ability by imposing scratches on the surface of glass mounted films. The damaged polymers were irradiated with 254 nm UV light to reduce the polymer to oligomeric material and the visual healing of the scratches monitored by optical microscopy.

As shown in Figure 5, a scratch of 34 µm width on the surface of polymer 4ACM-10 was seen to be healed at room temperature with a 4.80 J/cm^2 dose of 254 nm irradiation. Figure 6 shows polymer 4ACM-m was able to heal a 29 µm wide scratch with a 5.48 J/cm^2 dose of 254 nm irradiation also at room temperature. Unexpectedly the irradiation dose was very similar to that of the much more flexible 4ACM-10 polymer. This is likely due to the depolymerised T_g measured earlier, as the T_g of 4ACM-m was 18 °C lower than that of 4ACM-10. As both had depolymerised T_g values below room temperature, healing at room temperature was possible due to the depolymerised material being able to flow into the damage site. However, as the T_g of 4ACM-m is significantly lower it will flow faster and hence heal quicker. Unfortunately the more rigid 4ACM-6 polymer was not found to give the desired healing property. Although during monitoring of the healing of the surface scratch there was some evidence of healing, the scratches did not heal as completely as observed with the other two polymers (Figure S5). This is most probably due to the high rigidity of the polymer and the high depolymerised T_g that, as explained earlier, limits the ability of the depolymerised material to flow and hence the ability for the scratch site to be filled and healed.

As the photoreversible mechanism that gives rise to the healing is repeatable, it allows for repeatable healing of the polymer in the same region as the structure is reformed after each healing cycle, this ability was demonstrated with the 4ACM-m polymer and also displayed in Figure 6. The previously healed sample of 4ACM-m was repolymerised with a treatment of 16.5 J/cm^2 dose of 365 nm irradiation, which was 1.5x times the dose seen to give maximum repolymerised, then a 36 µm scratch was made perpendicular to the original healed scratch. The sample was then seen to be healed with a 10.9 J/cm^2 dose of 254 nm irradiation, which is double that of which was required for the healing of the initial scratch. This can be attributed to two factors: the second scratch is wider and more

Table 2: Vickers hardness (HV) measurement results for three states of the polymers.

	4ACM-6	4ACM-10	4ACM-m
Polymerised	33.1	18.3	25.8
Depolymerised	20.8	12.3	17.2
Repolymerised	31.3	17.0	24.5

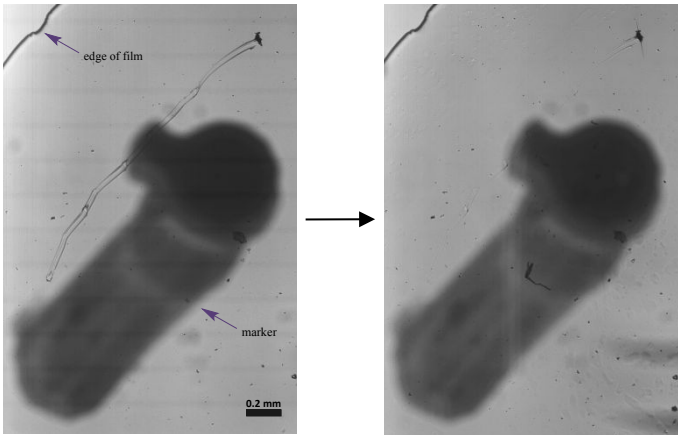

Figure 5: OM images of a 34 µm scratch on the surface of the polymer 4ACM-10 before (left) and after (right) irradiation with 254 nm light at room temperature.

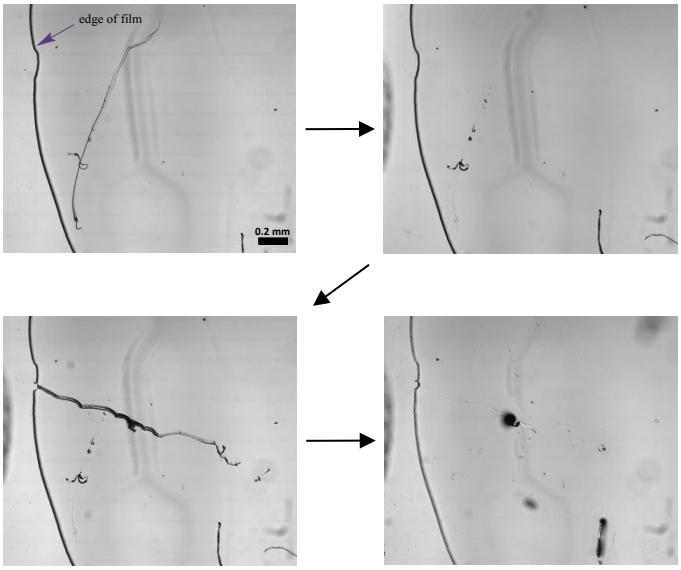

Figure 6: OM images of the 254 nm UV light induced healing of a scratch on the surface of polymer 4ACM-m and the subsequent repeatable healing of a second perpendicular scratch on the same sample, with scratch widths of 29 µm and 36 µm respectively.

severe than the original meaning that more material must be depolymerised and flow to the site to heal the damage and, to a much lesser extent, the imperfect reversibility seen in the photoreversibility study conducted earlier which showed the regain of 88% of the dimers and hence 88% of the potential dimers to cleave in the healing treatment to induce flow.

To ensure the healing response observed was due to the proposed photoreversible mechanism, and not just the heating effect of the continued irradiation, samples of each polymer were prepared and scratched, in a manner detailed above. However, in this instance the polymers were heated to 60 °C, which is much higher than the polymer would be exposed to during irradiation, and the scratch dimensions monitored. For all polymers there was no noticeable healing effect from this heating and hence the healing observed above can be attributed solely to effects arising from UV light exposure.

Conclusions

Through the synthesis of two new 4-armed coumarin monomers the creation of three photoreversible polymer systems was possible. By the UV light induced reversible dimerisation of the coumarin units the monomers were able to polymerise and depolymerise, giving rise to the desired photoreversible nature.

The polymers were characterised by a number of techniques to determine the structure and overall capabilities of the polymers. All three polymers were found to possess the thermal and mechanical properties required for the targeted coating application with the 4ACM-m polymer being produced to leverage the observed beneficial behaviour of each independent system. For example, the 4ACM-6 polymer had significant mechanical hardness but poor healing ability, while the more flexible 4ACM-10 polymer demonstrated exceptional healing but poor mechanical strength. When combined they formed the 4ACM-m polymer which had the healing ability of 4ACM-10 but superior mechanical properties. This leads to the possibilities to test different percentage mixtures to see the extent to which the 4ACM-6 percentage can be increased while still retaining room temperature healing ability.

The photoreversible character of these polymers gives rise to many potential applications other than self-healing. Such self-healing performance and photodegradation-induced solubility is indicative of the potential success for other applications that may leverage the photoreversible behaviour. The exceptional self-healing performance of the 4ACM-10 and 4ACM-m polymers represent, to our knowledge, the first photocurable coating material capable of room temperature self-healing.

Further research is thus being conducted into different uses of these photopolymers and potential structures of new monomers, in order to develop a more comprehensive suite of highly photoreversible polymers for different applications.

Conflicts of interest

There are no conflicts to declare.

Acknowledgements

The authors acknowledge the Chemicals and Plastics Manufacturing Innovation Network (C&PMIN) and training program (GRIP) curated by Monash University and supported by Chemistry Australia, the Victorian Government and 3M Australia. Dr Stefan Schmoelzer from Netzsch-Geraetebau GmbH Applications Laboratory (Wittelsbacherstrasse 42, 95100 Selb, Germany) for analysis of samples on their Photo-DSC 204 F1 Phoenix®. K. S. would like to thank the PRESTO, JST (JPMJPR1515), for financial support.

Notes and references

1 G. Oster and N.-L. Yang, *Chem. Rev.*, 1968, **68**, 125-151.
2 M. Hasegawa, *Chem. Rev.*, 1983, **83**, 507-518.
3 M. Kaur and A. K. Srivastava, *J. Macromol. Sci. Polymer Rev.*, 2002, **42**, 481-512.
4 Y. Heo, M. H. Malakooti and H. A. Sodano, *J. Mater. Chem. A*, 2016, **4**, 17403-17411.
5 S. R. Trenor, T. E. Long and B. J. Love, *Macromol. Chem. Phys.*, 2004, **205**, 715-723.
6 R. H. Aguirresarobe, L. Martin, N. Aramburu, L. Irusta and M. J. Fernandez-Berridi, *Progr. Org. Coating.*, 2016, **99**, 314-321.
7 P. Johnston, C. Braybrook and K. Saito, *Chem. Sci.*, 2012, **3**, 2301-2306.
8 W. M. Xu, M. Z. Rong and M. Q. Zhang, *J. Mater. Chem. A*, 2016, **4**, 10683-10690.
9 P. Johnston, M. T. W. Hearn and K. Saito, *Aust. J. Chem.*, 2010, **63**, 631-639.
10 N. Bai, K. Saito and G. P. Simon, *Polym. Chem.*, 2013, **4**, 724-730.
11 N. Bai, G. P. Simon and K. Saito, *RSC Adv.*, 2013, **3**, 20699-20707.
12 M. Abdallh, M. T. Hearn, G. P. Simon and K. Saito, *Polym. Chem.*, 2017, **8**, 5875-5883.
13 J. P. Menzel, B. B. Noble, A. Lauer, M. L. Coote, J. P. Blinco and C. Barner-Kowollik, *J. Am. Chem. Soc.*, 2017, **139**, 15812-15820.
14 D. E. Marschner, H. Frisch, J. T. Offenloch, B. T. Tuten, C. R. Becer, A. Walther, A. S. Goldmann, P. Tzvetkova and C. Barner-Kowollik, *Macromolecules*, 2018, **51**, 3802-3807.
15 C. Heiler, S. Bastian, P. Lederhose, J. P. Blinco, E. Blasco and C. Barner-Kowollik, *Chem. Commun.*, 2018, **54**, 3476-3479.
16 X. Xing, L. Li, T. Wang, Y. Ding, G. Liu and G. Zhang, *J. Mater. Chem. A*, 2014, **2**, 11049-11053.
17 C.-M. Chung, Y.-S. Roh, S.-Y. Cho and J.-G. Kim, *Chem. Mater.*, 2004, **16**, 3982-3984.
18 B. D. Fairbanks, S. P. Singh, C. N. Bowman and K. S. Anseth, *Macromolecules*, 2011, **44**, 2444-2450.
19 W. J. Choi, J.-S. Chung, J.-j. Kim, S.-K. Kim, S.-H. Cha, M. Park and J.-C. Lee, *J. Coat. Technol. Res.*, 2014, **11**, 455-459.
20 J. Ling, M. Z. Rong and M. Q. Zhang, *J. Mater. Chem.*, 2011, **21**, 18373-18380.
21 B. Zhu, N. Jasinski, A. Benitez, M. Noack, D. Park, A. S. Goldmann, C. Barner-Kowollik and A. Walther, *Angew. Chem. Int. Ed.*, 2015, **54**, 8653-8657.
22 K. K. Oehlenschlaeger, J. O. Mueller, J. Brandt, S. Hilf, A. Lederer, M. Wilhelm, R. Graf, M. L. Coote, F. G. Schmidt and C. Barner-Kowollik, *Adv. Mater.*, 2014, **26**, 3561-3566.

23 T. Gruendling, K. K. Oehlenschlaeger, E. Frick, M. Glassner, C. Schmid and C. Barner-Kowollik, *Macromol. Rapid Commun.*, 2011, **32**, 807-812.
24 G. L. Fiore, S. J. Rowan and C. Weder, *Chem. Soc. Rev.*, 2013, **42**, 7278-7288.
25 S. Y. An, S. M. Noh, J. H. Nam and J. K. Oh, *Macromol. Rapid Commun.*, 2015, **36**, 1255-1260.
26 C. J. Kloxin and C. N. Bowman, *Chem. Soc. Rev.*, 2013, **42**, 7161-7173.
27 J. Manhart, S. Ayalur-Karunakaran, S. Radl, A. Oesterreicher, A. Moser, C. Ganser, C. Teichert, G. Pinter, W. Kern, T. Griesser and S. Schlögl, *Polymer*, 2016, **102**, 10-20.
28 H. Frisch, D. E. Marschner, A. S. Goldmann and C. Barner-Kowollik, *Angew. Chem. Int. Ed.*, 2018, **57**, 2036-2045.
29 G. Kaur, P. Johnston and K. Saito, *Polym. Chem.*, 2014, **5**, 2171-2186.
30 M. V. Maddipatla, D. Wehrung, C. Tang, W. Fan, M. O. Oyewumi, T. Miyoshi and A. Joy, *Macromolecules*, 2013, **46**, 5133-5140.
31 P. Brennan and C. Fedor, in *Coatings Technology Handbook*, ed. D. Satas and A. A. Tracton, CRC Press, Florida, 2nd Edition, 2000, ch. 12, pp. 103-112.
32 A. Mustafa, *Chem. Rev.*, 1952, **51**, 1-23.
33 R. Anet, *Can. J. Chem.*, 1962, **40**, 1249-1257.
34 J. Ling, M. Z. Rong and M. Q. Zhang, *J. Mater. Chem.*, 2011, **21**, 18373-18380.
35 V. X. Truong, F. Li, F. Ercole and J. S. Forsythe, *ACS Macro Lett.*, 2018, **7**, 464-469.
36 V. X. Truong, F. Li and J. S. Forsythe, *ACS Macro Lett.,* 2017, **6**, 657-662.
37 R. Liu, X. Yang, Y. Yuan, J. Liu and X. Liu, *Progr. Org. Coating.*, 2016, **101**, 122-129.
38 M. Nagata and Y. Yamamoto, *React. Funct. Polym.*, 2008, **68**, 915-921.
39 E. Sato, S. Nagai and A. Matsumoto, *Progr. Org. Coating.*, 2013, **76**, 1747-1751.
40 Y.-L. Chen, C.-M. Lu, S.-J. Lee, D.-H. Kuo, I.-L. Chen, T.-C. Wang and C.-C. Tzeng, *Bioorg. Med. Chem.*, 2005, **13**, 5710-5716.
41 M. S. Lee and J.-C. Kim, *J. Appl. Polym. Sci.*, 2012, **124**, 4339-4345.
42 V. J. Lopata, C. B. Saunders, A. Singh, C. J. Janke, G. E. Wrenn and S. J. Havens, *Radiat. Phys. Chem.*, 1999, **56**, 405-415.
43 E. Lokensgard, *Industrial Plastics: Theory and Applications*, Cengage Learning, Boston, 2008.
44 P. Ray, T. Hughes, C. Smith, G. P. Simon and K. Saito, *ACS Omega*, 2018, **3**, 2040-2048.
45 M. Mathew, K. Shenoy and K. Ravishankar, *Int. J. Sci. Stud.*, 2014, **5**, 71-75.
46 J. Suwanprateeb, *Polym. Test.*, 1998, **17**, 495-506.
47 S. R. White, N. Sottos, P. Geubelle, J. Moore, M. R. Kessler, S. Sriram, E. Brown and S. Viswanathan, *Nature*, 2001, **409**, 794-797.
48 K. S. Toohey, N. R. Sottos, J. A. Lewis, J. S. Moore and S. R. White, *Nat. Mater.*, 2007, **6**, 581-585.
49 J. F. Patrick, K. R. Hart, B. P. Krull, C. E. Diesendruck, J. S. Moore, S. R. White and N. R. Sottos, *Adv. Mater.*, 2014, **26**, 4302-4308.
50 J. H. Xu, S. Ye, C. D. Ding, L. H. Tan and J. J. Fu, *J. Mater. Chem. A*, 2018, **6**, 5887-5898.
51 W. Wang, L. Xu, X. Li, Z. Lin, Y. Yang and E. An, *J. Mater. Chem. A*, 2014, **2**, 1914-1921.
52 T. Hughes, G. P. Simon and K. Saito, *Polym. Chem.*, 2018, **9**, 5585-5593.
53 S. Banerjee, R. Tripathy, D. Cozzens, T. Nagy, S. Keki, M. Zsuga, and R. Faust, *ACS Appl. Mater. Interfaces*, 2015, **7**, 2064–2072.

Highly photoreversible photo-curable crosslinked epoxy coatings that can heal substantial surface damage were formed by the synthesis of unique monomers.